

## EDMX Research Day 2026

3rd February 2026, 11:00 – 18:00, CO

Time	Session	Speaker – Presentation – Activity
10:30 – 11:00	<b>Registration and coffee</b>	Mounting of posters on pinboards
11:00 – 11:20	<b>Welcome &amp; Introduction</b>	<b>Prof. Esther Amstad</b> EDMX Program Director
11:20 - 11:40	<b>Talk</b>	<b>Dr Matteo Hirsch</b>
11:40 – 12:00	<b>Pitch talks</b>	1-minute talks by poster presenters (Public voting for prize)
12:00 – 13:15	<b>Lunch break &amp; Poster session 1</b>	Odd numbers
13:15 – 14:15	<b>Doctoral students talks</b>	<p><b>Julia Lorenzetti (501 - Materials for Energy Conversion)</b> Enhancing solid booster utilization in redox targeted flow batteries with non-fluorinated binders</p> <p><b>Ray Cowen (LRM)</b> (SENS)2 of calcium–silicate–hydrate: Probing the atomic-level surface structure of cements</p> <p><b>Ekaterina Poliukhina (SUNMIL)</b> Direct measurement of protein pair interaction potentials</p>
14:15 – 15:30	<b>Coffee break &amp; Poster session 2</b>	Even numbers
15:30 – 16:30	<b>Round table discussion with EDMX alumni</b>	<p><b>Dr Lorenz Hagelüken</b> <b>Dr Michele Bozzetti</b> <b>Dr Matteo Hirsch</b> <b>Dr Sophia Thiele</b></p>
16:30 – 17:00	<b>Prize awards &amp; Conclusions</b>	<b>Prof. Esther Amstad</b> EDMX Program Director
17:00 – 18:00	<b>Closing apéro</b>	

**Scientific Committee:** Dr Allison Chau (SMaL), Dr Julie Gheysen (LMM), Dr Deepika Sardana (SUNMIL), Dr Morgan Barbey-Binggeli (INE), Dr Calixe Bénier (TIC), Dr Javier Castillo Seoane (LMSC), Dr Ignacio Rodriguez Barber (LMM)

## Posters list (Posters marked with a \* are giving pitch presentations)

Number	Name	Poster Title
1*	Abdullah Aydemir	Improving high temperature properties of Hastelloy X through microstructure engineering and oxide dispersion strengthening
2	Adam Woodhouse	ABA Triblock Copolymer Hydrogels with Bio-inspired Physical Crosslinks
3	Aleksandr Poliukhin	Electron-phonon interactions beyond DFT
4	Anna Koptelova	Protein-Based Materials from Amyloid Fibrils: Composite Films and Multilayers
5	Anna Duvakina	Static and dynamic magnetic properties of corrugated NiFe thin films patterned by DNA-self-assembled nanotemplates.
6*	Annalena Erlacher	Pressure- and temperature-driven microstructural and grain boundary evolution in alumina
7	Anthony Hoogmartens	Enhancing reprocessability of dynamic polymer composites with thermally sensitive particles and controlled particle-matrix interfaces
8	Arslan Mazitov	Lightweight, universal machine-learning model for atomistic materials simulations
9	Atreyee Acharya	Multiscale characterization of failed bioprosthetic heart valves using X-rays
10	Axel Deenen	Superconducting Diode Effect in Hollow Superconducting Helices
11	Biruktait Ayele Lemecho	Integrating CO <sub>2</sub> Capture, Conversion to Methane in Compact Device for Mars In situ Propellant Production
12	Blanca de Miguel Martínez	Production of bio-based materials from fungal fermentation
13	Brian Ridenour	Bioinspired Design of Nano-Reinforced Granular Hydrogels
14	Bruno Ploumhans	Discretization Error Quantification in Plane-Wave Density Functional Theory
15	Buse Tatli	Influence of Glucose-Based Additives on Cellulose Nanocrystal Self-Assembly
16	Ceren Mitmit	Improving Voc in wide bandgap ACIGS solar cells
17	Claire Paetsch	First-principles thermodynamics of hydrogen absorption in binary C15 Laves phases
18	Damien Lee	Modeling the equilibrium vacancy concentration in multi-principal element alloys from first-principles
19	Deepak Somanı	First-principles models of defects in alloys
20	Ding Ren	Low-Density Lipoprotein Forming Corona: Characterization and Use in Cancer Detection
21*	Disha Bandyopadhyay	Self healing polymers for reconfigurable architected structures

<b>22</b>	Egor Rumiantsev	Including Long-Range Interactions and Electric Response in Machine Learning Potentials
<b>23</b>	Ekaterina Poliukhina	Direct measurement of protein pair interaction potentials
<b>24</b>	Etchevers Marjorie	Factors influencing early-age properties of clinker
<b>25</b>	Ferdinand Posva	Supercurrent in a lateral S/F/S Josephson junction incorporating NbTiN and Ni grown by atomic layer deposition
<b>26</b>	Filip Koldzic	Effect of Supramolecular End Group Dynamics on Bulk Relaxation in a High Molar Mass Polyester
<b>27</b>	François Rivat	Moisture-Initiated Crosslinking of 3D Printed Double-Network Granular Elastomers
<b>28</b>	Gaëtan Denis	Electro Sinter Forging Process and Properties
<b>29</b>	Guoyuan Liu	Beyond DFT: delta learning on transition-metal oxides
<b>30</b>	Hari Priya Ravindran	Thermodynamic kinetic modelling of calcium aluminium sulphates
<b>31</b>	Hendrik Jansen	When Interfaces Fail: Thermal Stability and Mechanical Consequences in Metal–Ceramic Nanocomposites
<b>32</b>	Hien Tran Thi	Repurposing virustatic Resveratrol into a broad-spectrum virucidal with elevated non-toxicity and anti-inflammation activities
<b>33</b>	Jean-Baptiste Desbrest	Process windows for debondable adhesives in high performance aerospace applications
<b>34</b>	Jinwon Song	Thermally Drawn Stretchable Optical Fibers
<b>35</b>	Joao Pedro Assuncao	Squaraine dye based organic photomultiplication diodes with 220% external quantum efficiency at 1240 nm
<b>36</b>	Julia Lorenzetti	Enhancing Solid Booster Utilization in Redox Targeted Flow Batteries with Non-Fluorinated Binders
<b>37</b>	Kamila Hamulka	Effects of strain rate and c-axis orientation on microscale $\alpha$ -Ti compression: From kink bands to twinning
<b>38*</b>	Kewei Zhou	Ultrafast Dynamics of Magnetic Flux Quanta in a Superconducting Ring
<b>39</b>	Kyle Haas	Unassisted Water Splitting with Earth-Abundant Semiconductors
<b>40</b>	Lianxin Xu	Optimized silane chemical vapor deposition for robust aptamer nanopore functionalization
<b>41*</b>	Lorenzo Piersante	Two-step nucleation lowers energy barriers for structural transformations in metallic alloys
<b>42</b>	Louis Gobber	THz control of diamond NV centers
<b>43</b>	Luca Righetti	Quantum embedding for strongly correlated defects in PAW calculations from the algorithmic inversion method
<b>44</b>	Maja Lopandic	Swelling Accelerated Reduction of Disulfide-Crosslinked Tetra-PEG Networks
<b>45</b>	Malo Hervé	Ultrafast Magnetic Fields from THz-Driven Chiral Phonons

<b>46</b>	Mario Caserta	xc-functional dependence of the local screened Coulomb interaction and the dynamical Hubbard functional
<b>47</b>	Martina Birocco	Assessing humidity-induced fracture toughness degradation in polycrystalline alumina
<b>48</b>	Matteo Darra	The Effect of Cellulose Surface Chemistry on Mycelium-Cellulose Nanofiber Composites
<b>49</b>	Matthias Kellner	Advances in chemical shielding predictions of organic solids
<b>50</b>	Michele Bonacina	Superhydrophobic coatings by UV-PIPS
<b>51</b>	Mohammad Mobasher	Phase transformations in recycling of waste concrete through thermal processing
<b>52</b>	Nataliya Paulish	Databases of Fermi surfaces and de Haas-van Alphen oscillation frequencies from first principles simulations
<b>53</b>	Nianduo Cai	Nanopore sensor-enabled single-molecule detection
<b>54</b>	Nicola Carrara	Enzyme-responsive nanofertilizer for sustainable agriculture
<b>55*</b>	Philipp Kroeker	Secondary Twinning and Twin-Twin Interaction Mechanisms of {11-21} deformation twins in Rhenium
<b>56</b>	Raphael Lemerle	Boosting Performance of Zn3P2/InP Heterojunction Solar Cells through Selective Area Epitaxy
<b>57</b>	Ray Cowen	(SENS)2 of calcium-silicate-hydrate: Probing the atomic-level surface structure of cements
<b>58</b>	Richa Rajadhyak	3D characterization of gas diffusion electrodes in CO <sub>2</sub> electrolyzers using electron microscopy
<b>59</b>	Robert Wojtaszczyk	Understanding the Contribution of Tricalcium Aluminate in the Early Strength Development of Portland Cements
<b>60</b>	Robin Studer	Salt Hydrate-Based Hydrogel Composite Materials for Energy Storage Applications
<b>61</b>	Rocio Garcia Montero	Room Temperature 3D Bioprinting of Functional Organoids
<b>62</b>	Samuel Bojarski	PVD/ALD Asymmetric Nanolaminates: Multilayer Libraries to Explore Thermal Stability of Cu-X Binary Alloys
<b>63</b>	Samuel Gatti	How to bring new battery materials to scale? Continuous production of carbon coated Na <sub>3</sub> V <sub>2</sub> (PO <sub>4</sub> ) <sub>3</sub>
<b>64</b>	Sandor Lipcsei	Nanoindentation Of Oxide Inclusions In Iron
<b>65</b>	Sebastian Niedermeyer	Analysis of Axial Hydrogen Diffusion and Hydride Precipitation in Zirconium Alloy Nuclear Fuel Claddings
<b>66</b>	Shixuan Shan	Variable Charge State, Magnetic Excitations, and Kondo-Effect of Sm/graphene/Ir(111)
<b>67</b>	Simone Cigagna	Forces within the dynamical Hubbard functional framework
<b>68</b>	Sneha Cheriyanparambil	Histidine-Rich Domain Mimics via Ring-Opening Polymerization of -Amino Acid N-Carboxyanhydrides
<b>69*</b>	Sudharsan Rathna Kumar	Quantifying the CO <sub>2</sub> Absorbed by Cement-Based Materials over their Lifetime

<b>70</b>	Suqiu Jiang	A Surface-Initiated Polymerization Strategy for the Controlled Synthesis of PDMS Brushes
<b>71</b>	Thanh Thi Ha Le	Glyoxylic Acid (GA)-Lignin as Paper Barrier Coatings for Food Packaging Applications
<b>72</b>	Timo Reents	Score-based diffusion models for accurate crystal-structure inpainting and reconstruction of hydrogen positions
<b>73</b>	Tushar Thakur	Novel fast Li-ion conductors for solid-state electrolytes from first-principles
<b>74</b>	Tyler Benkley	Numerical Simulations of an Additive Manufacturing Process
<b>75*</b>	Vahid Charkhesht	Graphene-based Supercapacitors: Bridging Energy and Power
<b>76</b>	William Le Bas	Explaining Interlayer Bonding of Additively Manufactured Aluminium through Fractography
<b>77</b>	Yameng Lou	The Effect of Ligands Randomness and Flexibility on Super-selective Multivalent Interactions
<b>78</b>	Yann Muller	First-Principles Thermodynamics of Multicomponent Alloys
<b>79</b>	Yuki Hayashi	Effect of Carbon Source Diversity on Mycelium's Structure and Mechanical Properties
<b>80</b>	Zoubeir Saraw	Mussel byssus-inspired spinning of ionically crosslinked fibers

# Enhancing Solid Booster Utilization in Redox Targeted Flow Batteries with Non-Fluorinated Binders

Julia Lorenzetti<sup>1,2</sup>, Paweł P. Ziemiański<sup>1</sup>, Cédric Kupferschmid<sup>1</sup>, David Reber<sup>1</sup>

<sup>1</sup>Empa, Swiss Federal Laboratories for Materials Science and Technology, Dübendorf, Switzerland

<sup>2</sup>EPFL, School of Engineering, Institute of Materials, Lausanne, Switzerland

The low energy density of redox flow batteries can be mitigated by incorporating solid capacity boosters in the electrolyte tanks. A redox mediator in solution (electrolyte) is charged/discharged in the electrochemical cell and pumped into the tank where it reacts chemically with the booster (solid electrode material). If this reaction is reasonably fast, the energy density of flow batteries can be improved manyfold due to the much higher charge storage capacity of solid electrode materials compared to dissolved active species. For example, lithium iron phosphate (LFP) was shown to be a suitable solid booster in combination with ferricyanide as a redox mediator.<sup>1</sup> Until now, polyvinylidene fluoride (PVDF) has been used as a binder in the manufacturing of booster pellets.<sup>2,3</sup> Amid growing concerns and tightening regulations surrounding PFAS compounds, we extruded LFP pellets with the non-fluorinated binder polycaprolactone (PCL) and screened their reaction rates using on-line UV–Vis spectroscopy. By replacing PVDF with PCL, the reaction rate between LFP and ferricyanide increased from 19% to 55% of LFP converted per hour. The increased rate can be explained by the lower hydrophobicity of PCL, determined by contact angle analysis. Non-fluorinated LFP boosters also exhibited improved capacity utilization during charge–discharge cycling in a symmetric flow battery, reaching nearly 100% at 1 mA cm<sup>-2</sup> compared to 85% for PVDF at the same current density. We demonstrate that replacing PVDF with non-fluorinated binders in solid booster composites offers a simple and immediately applicable strategy to improve both the efficiency and sustainability of aqueous RTFBs.

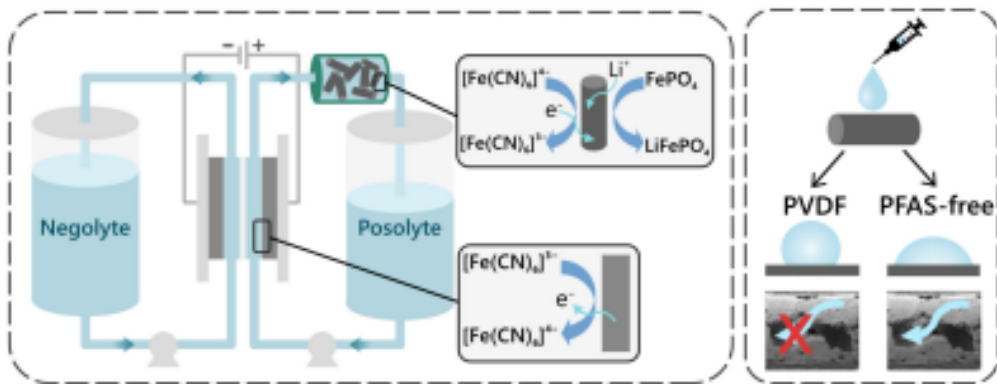


**Fig. 1:** Schematics of a redox targeted flow battery (left) and contact angle of water on a booster composite depending on binder (right).<sup>4</sup>

## References

- (1) Vivo-Vilches, J. F. *et al.* *J. Power Sources* **2021**, *488*, 229387. DOI: 10.1016/j.jpowsour.2020.229387.
- (2) Lotenberg, T. *et al.* *J. Power Sources* **2024**, *602*, 234290. DOI: 10.1016/j.jpowsour.2020.229387.
- (3) Marin-Tajadura, G. *et al.* *Adv. En. Mater.* **2025**, *15*(19). DOI: 10.1002/aenm.202404501.
- (4) Lorenzetti, J. *et al.* submitted.

# (SENS)<sup>2</sup> of calcium–silicate–hydrate: Probing the atomic-level surface structure of cements

X. Ray Cowen,<sup>1,2</sup> Tristan Georges,<sup>1</sup> Karen Scrivener,<sup>2</sup> Lyndon Emsley<sup>1</sup>

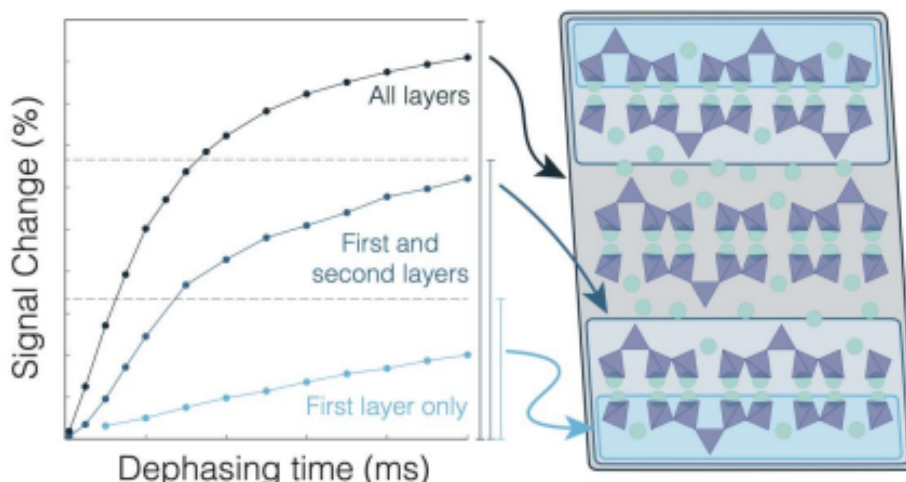
<sup>1</sup>Laboratory of Magnetic Resonance, Institut des Sciences et Ingénierie Chimiques

<sup>2</sup>Laboratory of Construction Materials, Institut des Matériaux

Cements are a major source of anthropogenic CO<sub>2</sub> emissions, driving a need to develop alternatives to carbon-intensive components. These alternatives, however, tend to weaken the primary binding phase, calcium silicate hydrate (C–S–H). A detailed understanding of the surface structure of C–S–H at the atomic-level, in particular, is crucial in developing insights to control the hydration reaction as well as mechanical and chemical properties.

Nuclear magnetic resonance (NMR) spectroscopy has proven to be a powerful tool in the atomic-level study of C–S–H; from its first use in the 1980s,<sup>1</sup> to the observation of the later stages of the hydration reaction<sup>2</sup> or the determination of the bulk structure of C–S–H.<sup>3</sup> However, while the bulk structure of C–S–H is well-characterized at the atomic level, direct experimental probes of the surface structure remain elusive. The extremely thin nature of C–S–H (~5 nm), and the ubiquity of hydrogen atoms throughout the structure, makes the application of even traditional surface-selective NMR techniques challenging.

Here, for the first time, we experimentally differentiate the surface structure from the bulk using new surface-enhanced NMR methods. With the isotopic selectivity of NMR and selective deuteration near the surface of the C–S–H, we are able to isolate NMR signals from silicate units originating at exclusively the surface of the material, thus allowing for characterization of the surface structure and comparison to the bulk. This breakthrough allows for analysis of the surface of C–S–H and its variants to uncover connections between atomic structure and macro-scale properties, a crucial step in the development of low-carbon cements



## References

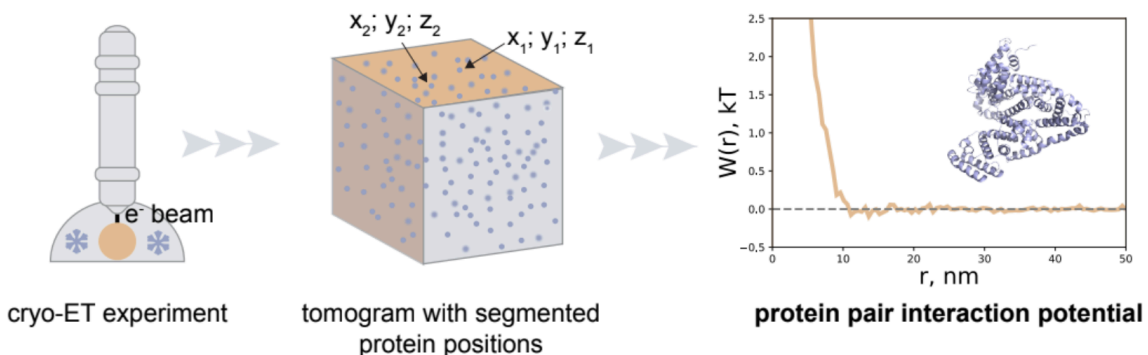
- [1] *Cem. Concr. Res.* **1982**, *12*, 333-339.
- [2] *Cem. Concr. Res.* **2004**, *34*, 857-868.
- [3] *J. Phys. Chem. C* **2017**, *121* (32), 17188-17196.

# Direct measurement of protein pair interaction potentials

E. Poliukhina,<sup>1</sup> Q. K. Ong,<sup>1</sup> and F. Stellacci<sup>1,2</sup>

<sup>1</sup>*Institute of Materials, Ecole Polytechnique Fédérale de Lausanne (EPFL), Lausanne, Switzerland* <sup>2</sup>*Bioengineering Institute, Ecole Polytechnique Fédérale de Lausanne (EPFL), Lausanne, Switzerland* e-mail: [ekaterina.poliukhina@epfl.ch](mailto:ekaterina.poliukhina@epfl.ch)

A direct and unambiguous method for obtaining protein pair interaction potentials (PIPs) does not currently exist. All available approaches require solving an inverse problem, which can allow for multiple solutions. Here, we report a straightforward method to obtain the PIP directly from experimentally determined three-dimensional protein spatial distributions. Our approach builds on improvements to a recently developed cryogenic electron tomography (cryo-ET) framework for determining the potential of mean force for nanoparticles [1]. For protein PIPs, we find strong agreement between the structure factor computed from cryo-ET positions and that obtained by small-angle X-ray scattering (SAXS) of protein solutions. We further introduce a novel sub-volume method to compute Kirkwood–Buff integrals and show that second virial coefficients derived from cryo-ET tomograms closely match those measured by analytical ultracentrifugation. Together, these results validate our approach for deriving the PIP and indicate that the vitrified state faithfully reflects the solution state. We demonstrate the generality of this method across several small proteins with distinct structures and molecular weights under varied experimental conditions, including changes in salt concentration, temperature, and pH. As an example, we show that adding amino acids can shift the PIP from a net-attractive to a fully repulsive regime, consistent with our recently published theoretical framework describing amino-acid-driven stabilization mechanisms [2]. Finally, we will present a novel extension of the method to capture the role of anisotropic protein interactions.



## References

- [1] Q. Ong, T. Mao, N. Iranpour Anaraki, Ł. Richter, C. Malinverni, X. Xu, F. Olgiati, P. H. J. Silva, A. Murello, A. Neels, D. Demurtas, S. Shimizu, F. Stellacci. *Mater. Horiz.* (2022) 9 (1), 303–311.
- [2] Mao, T., Xu, X., Winkler, P.M. et al. Stabilizing effect of amino acids on protein and colloidal dispersions. *Nature* (2025) 645, 915–921.